

STIC-ILL

QH506.E3

From: Huynh, Phuong N.
Sent: Tuesday, June 18, 2002 1:43 PM
To: STIC-ILL
Subject: RE: 09/761,636

YMC

Please deliver the following:

Please deliver the following:

J Biol Chem 266: 10073-77; 1991

J Biol Chem 267: 11260-66, 1992

J Biol Chem 269: 32879-85; 1994

Biochem Biophys Acta 1246: 1-9; 1995

EMBO J 11: 3921-26; 1992

Molecular and cell biology 13: 4066-76; 1993

Growth factors 7: 53-64; 1992

Methods in Enzymol 154: 367-82; 1987

Thanks,
Neon
Art unit 1644
Mail 9E12
Tel 308-4844

Crystal structure of human platelet-derived growth factor BB

C.Oefner¹, A.D'Arcy, F.K.Winkler, B.Eggimann and M.Hosang

Departments of Pharmaceutical Research—New Technologies and Preclinical Research and Development, F.Hoffmann-La Roche Ltd, CH-4002 Basel, Switzerland

¹Corresponding author

Communicated by J.N.Jansonius

The crystal structure of the homodimeric BB isoform of human recombinant platelet-derived growth factor (PDGF-BB) has been determined by X-ray analysis to 3.0 Å resolution. The polypeptide chain is folded into two highly twisted antiparallel pairs of β-strands and contains an unusual knotted arrangement of three intramolecular disulfide bonds. Dimerization leads to the clustering of three surface loops at each end of the elongated dimer, which most probably form the receptor recognition sites. Key words: platelet-derived growth factor/receptor binding domains/X-ray structure

Introduction

Platelet-derived growth factor (PDGF) represents the major serum mitogen for cells of mesenchymal origin. It has been shown to promote cell migration *in vivo* (Gordon *et al.*, 1991) and cell migration and proliferation *in vitro* (Kohler and Lipton, 1974; Ross *et al.*, 1974). Both are key events in natural processes such as embryogenesis and wound repair (Heldin and Westmark 1984; Ross *et al.*, 1986). PDGF has also been implicated in a number of pathological states, such as neoplasia, arteriosclerosis and fibrosis (Waterfield *et al.*, 1983; Ross *et al.*, 1986). The potent mitogenic, chemoattractant and transforming activities of PDGF are mediated through its interaction with specific high-affinity cell surface receptors (Heldin and Westmark 1989; Matsui *et al.*, 1989), leading to the stimulation of the receptor's intrinsic tyrosine-specific kinase activity (Gelmann *et al.*, 1981; Robbins *et al.*, 1981, 1982a,b; Wong-Staal *et al.*, 1981).

PDGF is a disulfide-linked dimeric protein, variably composed of two related polypeptide chains A and B, which are expressed from different genes and assembled as homo- or heterodimers (Johnsson *et al.*, 1982). Unreduced, active PDGF exhibits multiple forms ranging in size from 28–35 kDa (Antoniades *et al.*, 1979; Deuel *et al.*, 1981). Reduction of PDGF produces inactive, smaller peptides with apparent molecular weights of 12–18 kDa (Antoniades *et al.*, 1979; Heldin *et al.*, 1979). All three possible isoforms of PDGF, AA, BB and AB, have been identified and shown to bind with different affinities to homo- and heterodimers of two different but homologous receptor gene products, denoted α and β (Yarden *et al.*, 1986; Matsui *et al.*, 1989). According to the PDGF receptor subunit model (Seifert *et al.*, 1989), PDGF-BB activates all three receptor isoforms,

whereas PDGF-AA exclusively activates the αα dimer (Antoniades *et al.*, 1979; Kaplan *et al.*, 1979). The heterodimeric ligand activates both, the αα-dimer and the β-receptor subunit of a non-covalently linked αβ heterodimer (Heideran *et al.*, 1991; Kanakaraj *et al.*, 1991). Some predictions of this model have been recently questioned (Drozdoff and Pledger, 1991). PDGF-BB has been identified as the human homologue of the *v-sis* oncogene product p28^{sis} of the Simian Sarcoma virus (Dolittle *et al.*, 1983; Waterfield *et al.*, 1983), a transforming, replication-defective retrovirus, which was isolated from a naturally occurring fibrosarcoma in a woolly monkey (Theilen *et al.*, 1971; Waterfield *et al.*, 1983). This finding provided the first evidence that *onc* gene products were involved in growth factor-mediated proliferative pathways. Both proteins have in common a minimal transforming domain, containing eight cysteine residues, four of which are essential for PDGF function and have been inferred in intrachain disulfide linkages (Giese *et al.*, 1987; Sauer and Donoghue, 1988). We report here on the three-dimensional structure of recombinant human PDGF-BB at 3 Å resolution, determined by the multiple isomorphous replacement method. Taking into account biological data on the functional importance of single residues or of selected chain fragments of the ligand, a putative receptor binding site is proposed.

Results

Crystallography

The crystal structure of PDGF-BB has been determined by the multiple isomorphous replacement (MIR) technique at 3.2 Å and refined to the diffraction limit of the crystals. Refinement was performed using the fast Fourier version of the PROLSQ (Hendrickson and Konnert, 1980) program as implemented in the CCP4 software package (Daresbury Laboratory, England). Statistical information on data collection, MIR phasing and structure refinement is summarized in Table I. The refinement of PDGF-BB was not satisfactory until an overall anisotropic tensor was applied to the calculated structure factors of the isotropically refined protein structure following the approach of Sheriff and Hendrickson (1987). By assigning a vibrational tensor to the entire unit cell, constrained to have 2/m point group symmetry, the adverse effects of the highly anisotropic intensity distribution on the refinement process were essentially removed. Despite the moderate resolution of 3.0 Å, individual atomic B-factors were refined, albeit with tight restraints between covalently linked atoms. The three crystallographically independent PDGF-B molecules 1, 2 and 3 have mean main-chain B-values of 13 Å², 32 Å² and 35 Å², respectively, indicating a higher mobility of molecules 2 and 3 in the crystal lattice. As shown in Table I the highly anisotropic thermal ellipsoid has its largest component along the monoclinic b axis. Ideally an anisotropic tensor should be applied to each of the three independent molecules during

Table I. Statistics for data collection, phase determination and refinement

Derivative	Native	EuCl ₃	K ₂ PtI ₄
a) Diffraction data			
Number of measurements (No. of crystals)	24377 (3)	14512 (1)	14135 (1)
Number of unique reflections (completeness %)	8545 (99)	6921 (80)	4480 (92)
Resolution limit (Å)	3.0	3.2	3.65
R _I * (overall)	0.061	0.089	0.049
R _I (-6.32 Å)	0.054	0.083	0.040
R _I (6.32 Å–4.47 Å)	0.057	0.082	0.050
R _I (4.47 Å–3.65 Å)	0.064	0.089	0.068
R _I (3.65 Å–3.16 Å)	0.083	0.156	
R _I (3.16 Å–2.83 Å)	0.126	0.288	
r.m.s. F _h /E [†]			
(all reflections/highest resolution range)		3.0/1.8	1.5/1.1
R _C (only h0l) [‡]		0.38	0.56
Mean figure of merit	0.54 for 6,183 reflections		
b) refinement parameters			
No. of atoms (non-hydrogen)	2,037	Overall anisotropic thermal parameters (Å ²)	
r.m.s. deviation of bond length (Å)	0.02	b11	3.7 along a*
r.m.s. deviation of bond angles (degrees)	2.5	b22	14.1 along b*
Resolution	6.0–3.0 Å	b33	–2.3 along c*
No. of F _{obs} >= 3σ F _{obs}	6,172	b13	0.7
R-factor	0.209		

^{*}R_I = Σ|I – <I>| / Σ<I>[†]F_h heavy atom structure factor; E residual lack of closure[‡]Cullis R-factor = Σ|F_{h(obs)} – F_{h(calc)}| / Σ F_{h(obs)}

refinement, but this option is not yet implemented in the refinement software. Molecules 1 and 2 are related by a non-crystallographic 2-fold axis, while molecule 3 is part of a crystallographic dimer. The crystal packing can be described as a stacking of layers along the b-axis. Each layer consists of dimers of both types (1/2 and 3/3) that contact each other in the a,c plane. The interlayer contacts are relatively weak and occur exclusively between molecules of type 1 related by the 2-fold screw operation. This explains the observed higher mobility of molecules 2 and 3 and also that the largest component of this mobility is along the b-axis. The present crystallographic R-factor with all molecules refined independently is 20.9% for data with F/σ_F > = 3 and reflections in the resolution range 6.0–3.0 Å. r.m.s. deviations from ideal bond length and angles are 0.02 Å and 2.5°, respectively. Figure 1 shows the initial MIR electron-density distribution and the final 2|F_{obs}| – |F_{calc}| map, calculated with model phases, for a prominent feature of the monomeric PDGF-B structure, a cluster of three disulfides.

Molecular structure

The polypeptide chain fold of a monomeric PDGF-B molecule is shown in Figure 2a together with the assignment of secondary structure elements. Mature human PDGF-B has 109 amino acids (Josephs *et al.*, 1984), which correspond to residues 82–190 of the PDGF-B precursor and to residues 112–220 of the *v-sis* gene product p28^{sis} (for residue numbers referring to the *v-sis* gene product p28^{sis} the corresponding mature PDGF numbers will be indicated in square brackets). The molecule belongs to the class of β-proteins and has two long, highly twisted antiparallel pairs of β-strands as also seen in the crystal structure of nerve growth factor (McDonald *et al.*, 1991). The strand connections, denoted as loops I, II and III, range from residues Ile25–Leu38, Cys53–Val158 and

Val78–Lys81, respectively, are exposed to solvent and show partial disorder in all three independent monomers. This is also the case for the N- and C-termini and will obviously be aggravated for loop I and the N-terminal end by the presence of a substantial fraction of nicked molecules, as discussed below. As a consequence 6–8 N-terminal residues, 5–9 C-terminal residues as well as the fragment 28–36 are missing in the structural model of the three monomer copies. A prominent feature of the PDGF-B molecule is an intramolecular cystine cluster, located in the region of loop II (see Figure 1), which is formed by the three disulfides Cys16–Cys60, Cys49–Cys97 and Cys53–Cys99. They are arranged in an unusual knot-like topology with the Cys16–Cys60 bridge (I–IV) penetrating the cyclic structure formed by the two other cystines (II–V and III–VI) and their strand connections. A similar knotted arrangement of disulfide bonds has been observed in a number of structurally related proteins, with the same I–IV, II–V, III–VI intramolecular cystine network. These are the trypsin inhibitor EETI II (Le Nguyen *et al.*, 1990) from *Ecbalium elaterium*, CPI, a carboxypeptidase inhibitor found in potato leaves (Rees and Lipscomb, 1982) and the neurotoxin ω-canotoxin GVIA from *Conus geographus* (Nishiuchi *et al.*, 1986). However, their cystine topology differs from that of the PDGF-B monomer as in these cases the disulfide bridge III–VI penetrates the macrocycle. Strikingly, there is a close structural resemblance in the main-chain fold between loop II (residues Cys53–Val58) and the corresponding region (Cys12–Asp17) of the carboxypeptidase A inhibitor CPI (4CPA). Their equivalent C_α-positions superimpose with an r.m.s. deviation of 0.4 Å, thus representing a conserved loop motive in the presence of the knot-like cystine topology. The two remaining cysteine residues of PDGF are involved in interchain disulfide linkages. Cys43 forms a disulfide bridge with Cys52 of the

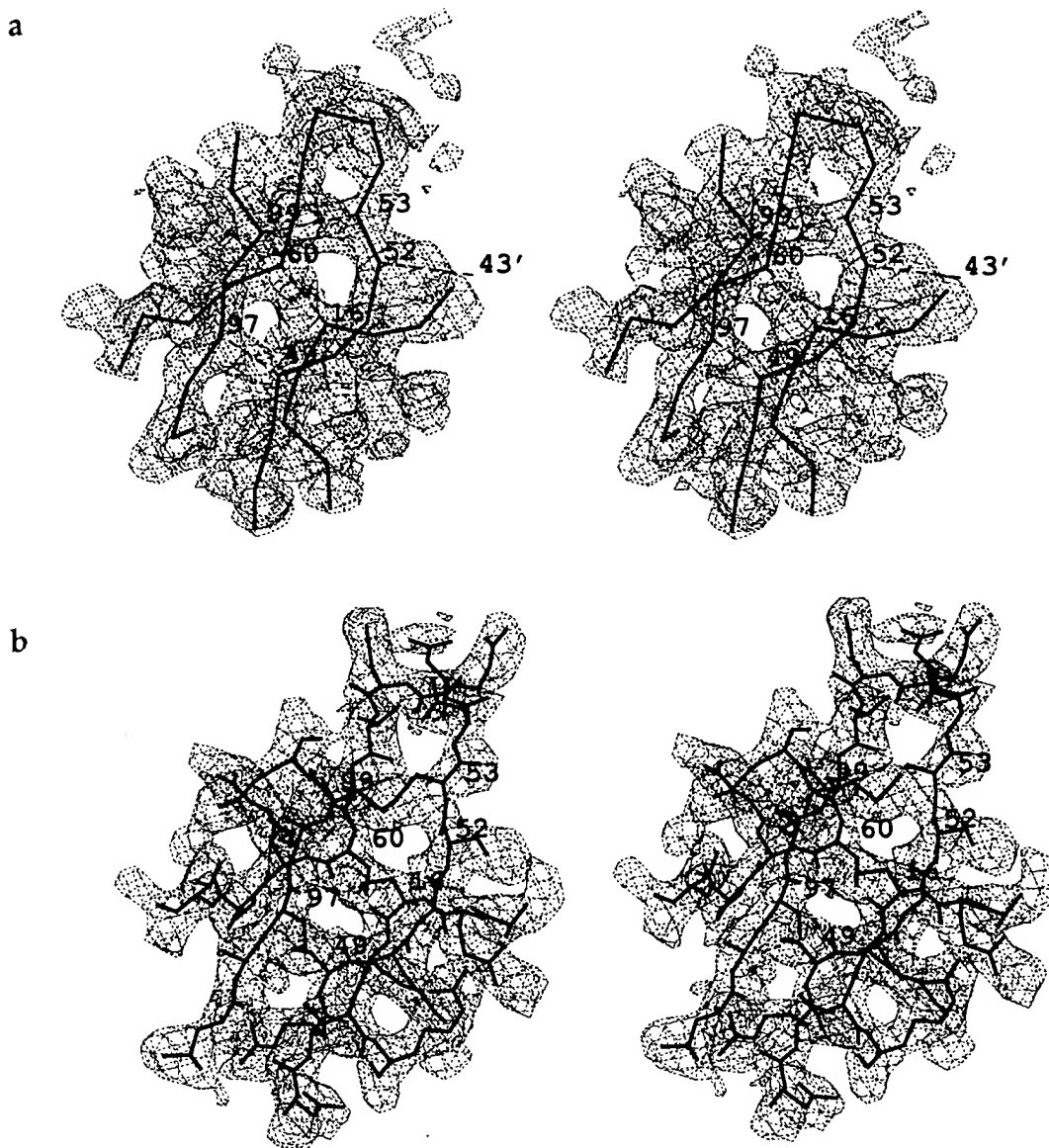


Fig. 1. Stereo representation of the initial MIR electron density distribution (a) and the final $2|F_O| - |F_C|, \alpha_c$ -map (b) for the intramolecular cystine cluster Cys16–Cys60, Cys49–Cys97 and Cys53–Cys99. Superimposed on the displayed densities are for (a) the corresponding portions of the C_α -chain (disulfide bonds indicated in dashed lines) and for (b) the refined structure.

symmetry related chain and vice versa, giving rise to the ‘antiparallel’ dimer arrangement of the elongated monomers as shown in Figure 2b in two different orientations. Viewed on edge the PDGF dimer has the shape of a shallow trough with overall dimensions of $\sim 70 \times 35 \times 25 \text{ \AA}$. The main body is exclusively formed by β -strands whereas the two ends are formed by the C-termini and the surface loops I, II and III. One part of the dimer interface extends over almost 40 \AA parallel to the direction of β_1 and β_2 and is formed predominantly by van der Waals contacts between residues of both strands with their symmetry related copies. As can be seen from Figure 2b additional intermolecular contacts are formed by the N-terminal tails (residues 7–15). They cross the extended part of the interface near the intermolecular disulfide bonds on the convex side of the dimer. The calculated solvent-accessible surface area of both the non-crystallographic dimer and the individual monomers shows that $\sim 2200 \text{ \AA}^2$ of the total surface area are buried in the dimer. Of these $2 \times 600 \text{ \AA}^2$ can be attributed to the contacts made by the N-termini over a distance of $\sim 18 \text{ \AA}$.

Approximately $2 \times 500 \text{ \AA}^2$ are buried along the extended $\beta_1\beta_2$ interface, including the contact at the intermolecular disulfide bond.

Discussion

Disulfide linkages

Studies with deletion mutants of the *v-sis* gene product demonstrated that the minimal region required for transforming activity contains all of the conserved cysteines and corresponds to the chain segment Cys16–Cys99 in the mature PDGF-B molecule (Giese *et al.*, 1987). All cysteine residues in PDGF were reported to be involved in either inter- or intramolecular disulfide linkages (Deuel *et al.*, 1981) and reduction of PDGF or the *v-sis* protein abolishes mitogenic activity (Deuel *et al.*, 1983; Garrett *et al.*, 1984; Huang *et al.*, 1984; Owen *et al.*, 1984). This indicated a crucial role of some or all disulfide bonds in the stabilization of the biologically active conformation and suggested that a dimeric ligand structure might be functionally important.

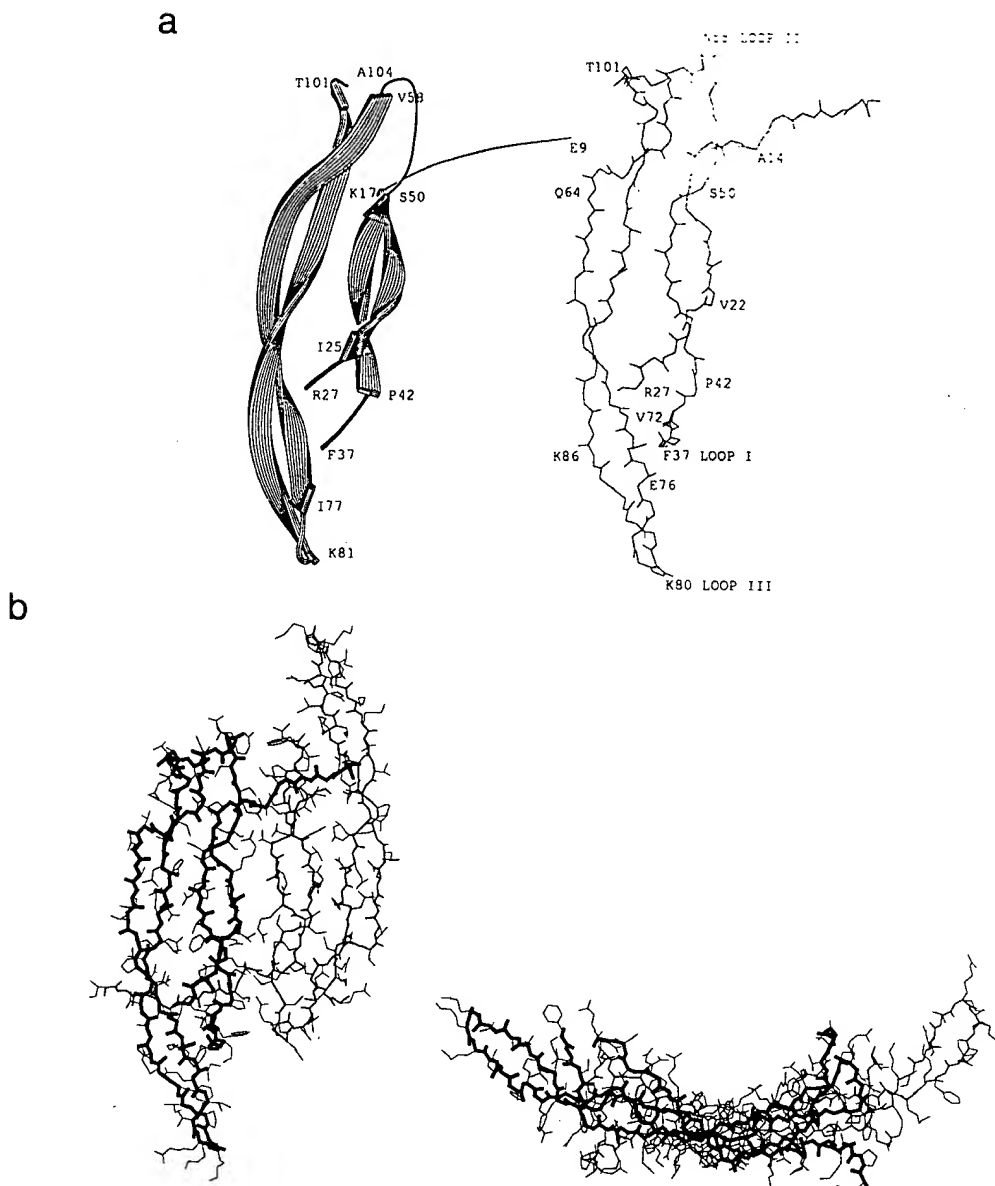


Fig. 2. (a) Backbone structure of the refined monomeric PDGF-B-chain (A9-A104) represented as a ribbon diagram (Priestle, 1988) (left) and a wire model (right). Secondary structure elements have been assigned using the algorithm of Kabsch and Sander (1983). The residues indicated in the ribbon diagram mark the N- and C-termini, the beginning and end of each β -strand and the break points of the missing loop. (b) Atomic structure of the refined non-crystallographic disulfide-linked PDGF-BB dimer viewed along the approximate 2-fold axis (left) and edge on (right). Molecules 1 and 2 are drawn in thick and thin lines, respectively.

Given the importance of the disulfide bonds for the ligand's biological activity, the structural and functional role of individual cysteine residues in the PDGF related *v-sis* oncogene has subsequently been probed with Cys to Ser mutants (Giese *et al.*, 1987; Sauer and Donoghue, 1988). It was found that the cysteine residues 127, 160, 171 and 208 (16, 49, 60 and 97 in the mature PDGF-BB sequence) are essential for transforming activity and it was correctly concluded that they are involved in intrachain disulfide linkages. However, the connectivity of these linkages could not be derived. The remaining four cysteines 154, 163, 164 and 210 [43, 52, 53 and 99] could be replaced by serine without loss of biological activity. Furthermore, it was suggested that Cys154 [43] and Cys163 [52] participate in a non-essential intra- or intermolecular disulfide bridge (Sauer and Donoghue, 1988). The intermolecular disulfide bond between Cys43 and Cys52 of mature PDGF as well

as the third intramolecular cysteine Cys53–Cys99 can thus be regarded as functionally non-essential.

Substitution of Cys163 [52] by serine did not reduce biological activity but altered the electrophoretic mobility under non-reducing conditions (Giese *et al.*, 1987). This was interpreted as an indication for biological activity of a monomer or of a non-covalently linked dimer. Indeed, the structure shows that the dimer interface is sufficient to substantially stabilize a dimer in the absence of a covalent linkage. However, the minimal transforming domain, which lacks the N-terminal 15 residues and their significant contribution to the dimer interface, is likely to remain monomeric at low concentration.

Receptor binding domains

Identification of those regions of PDGF-BB that are involved in the binding to or in the activation of the receptor's intrinsic

tyrosine kinase activity is of particular interest for the design of specific PDGF antagonists. A number of studies, using deletion and substitution mutants of PDGF-B or of the homologous *v-sis* gene as well as PDGF-A/B chimeras provided some insights (LaRochelle *et al.*, 1989, 1990; Giese *et al.*, 1990; Clements *et al.*, 1991; Östman *et al.*, 1991). A more precise description of the binding domains is now possible through the knowledge of the location of the functionally important residues in the three-dimensional structure of the ligand.

Initial studies with neutralizing PDGF monoclonal antibodies (LaRochelle *et al.*, 1989) indicated that the chain segment between Thr20 and Cys43 represents a surface domain of PDGF-BB and contains residues involved in receptor interaction. More precise epitope mapping and site directed mutagenesis studies with *v-sis* further confined this binding domain to residues Ile136 [25]–Phe148 [37] (Giese *et al.*, 1990). Using PDGF-A/B chimeras it was shown that Asn34 is essential for PDGF-B-like transforming efficiency (Östman *et al.*, 1991). Using a different functional assay, which selects for mutants with reduced binding to both receptor types, Ile30 and to a lesser extent Arg27 were shown to be important (Clements *et al.*, 1991). *v-sis* mutants with single residue deletions in the segment corresponding to loop I lack transforming activity but show no reduction in dimer formation (Giese *et al.*, 1990). Most likely, this loop assumes a defined structure only when PDGF binds to its receptor. In the free ligand it is flexible and seems to adapt to sequence alterations without disturbing the rest of the molecular structure and therefore dimerization. It should be noted that single residue deletions in the more rigid parts of the molecule lead to the loss of transforming activity and dimer formation.

The 2-fold symmetry of PDGF-BB leads to a clustering of all three loop regions on either end of the dimeric molecule. Despite the lack of interpretable density for loop I, it must be in close proximity to loop III of the same monomer and to loop II of the 2-fold related molecule. Given the high affinity of PDGF-BB for its receptors (Bowen-Pope and Ross, 1982), an extended interaction interface, likely to include regions spatially adjacent to loop I, may be expected. Indeed, one study with PDGF-A/B chimeras (Östman *et al.*, 1991) strongly indicates that residues from segment 73–77, most likely Arg73 and Ile77, are involved in β-receptor binding. Somewhat contradictory, Giese *et al.* (1990) reported that residues Glu24–Thr63 of the B-chain confer full B-like functional properties to A/B chimeras. As pointed out by Östman *et al.* (1991), the conflicting results may be a consequence of the different systems used for the functional assays. The structure shows that the extended segment 73–77, just before loop III, is adjacent to loop I and that the side chains of Arg73, Ile75 and Ile77 participate in a large, predominantly hydrophobic patch that also includes Arg27, Leu38 (both part of loop I), Pro82 and Phe84. This non-polar pattern is conserved in the human PDGF-A sequence.

Positively charged amino acid residues have been attributed an important role in the binding of PDGF-BB to its receptors from the finding that protamine (sulfate), a highly basic (Arg- and Lys-rich) polypeptide is a competitive inhibitor of PDGF binding (Huang *et al.*, 1982). Interestingly, loop III (Val78–Arg79–Lys80–Lys81) contains three basic residues that are conserved in the human

A and B chains. However, their substitution by neutral or acidic residues has been shown to have no effect in the functional assay that probes reduced binding to both receptor types (Clements *et al.*, 1991). With respect to an involvement of loop II residues, it can be said that closest to the ordered ends of loop I are Asn55, Arg56 and Asn57. No data on the functional importance of loop II residues are available, with the exception that Arg56 has been probed and found not to be important in the assay probing binding to both receptor types (Clements *et al.*, 1991).

In summary, the fragmented biological data on the functional importance of particular residues of PDGF-B combined with the structural results suggests to us that residues of loop I possibly together with mainly non-polar residues on the N- and C-terminal side of loop III and perhaps additional residues from a dimer related loop II could form an extended contiguous receptor binding site. Further biological and structural results will be necessary to confirm or modify this hypothesis.

Materials and methods

Purification and crystallization

The clone bearing the plasmid PKP36, expressing human B-chain PDGF, was grown in *S. cerevisiae* E-18-9 strain yeast cells (Kelly *et al.*, 1985) in 100 l fermenters. The yeast culture broth, containing the secreted PDGF-BB, was centrifuged and the supernatant concentrated using polysulfone membranes (Millipore) with a 10 000 M.W. cut-off. The pH was adjusted to 5.5 and 10 mM EDTA added before loading onto S-sepharose FF. PDGF was eluted with a step gradient of 1 M NaCl in 20 mM phosphate buffer at pH 7.3. As PDGF is extremely stable at low pH, the pH was lowered to 3.0 with acetic acid and the protein rechromatographed on S-sepharose FF, using an acetic acid sodium acetate gradient from pH 3.0 to 5.0. The protein was then concentrated using Amicon YM10 membranes and applied to a G-50 gel filtration column in 1 M ammonium acetate buffer at pH 9.0. The pH of the peak fractions was adjusted to 4.5 with acetic acid and subsequently diafiltered with water to reduce the salt concentration before lyophilization. An orthorhombic crystal form, grown from 50% isopropanol tended to be twinned and relatively few crystals were suitable for data collection. A monoclinic form, grown in 25% isopropanol, 25% PEG 400, 250 mM CaCl₂ and 20 mM HEPES, pH 7.0 showed no twinning, could be grown reproducibly and was used for x-ray analysis. Calcium chloride proved to be essential for their growth and a protein concentration of 40 mg/ml was necessary to produce crystals large enough for data collection. The crystals belong to space group C2 ($a = 147.3 \text{ \AA}$, $b = 31.8 \text{ \AA}$, $c = 90.1$, $\beta = 98.7^\circ$), contain three molecules in the asymmetric unit and diffract to a spacing of 3 Å. They have been obtained using standard vapour diffusion techniques in hanging drops (McPherson, 1976) at room temperature. For soaking native crystals were transferred to a buffer containing 50% PEG 400, 125 mM CaCl₂ and 20 mM HEPES, pH 7.0. N-terminal sequence analysis of the purified material shows that ~50% of the B-chains are nicked either between residues Leu5–Thr6 and/or Arg32–Thr33. The purification procedure for PDGF-BB does not separate dimers with two intact chains from those with one or two nicked polypeptides. This heterogeneity is also present in the crystallized material as apparent from SDS gel electrophoresis (data not shown).

Crystallographic analysis

Diffraction data were recorded by a Siemens/Nicolet area detector, installed on an Elliot GX-21 rotating anode generator operated at 40 kV, 80 mA and equipped with a graphite monochromator. Data frames of 0.1° and 0.2° with exposure times between 90 and 120 s were collected and processed with the XDS software (Kabsch, 1988). All subsequent crystallographic calculations were performed using the CCP4 software package (obtained from Daresbury, England). An isomorphous low resolution difference Patterson could be solved for a SmCl₃ derivative. Four sites were identified and SIRAS phases, obtained from the single isomorphous and anomalous differences, were used to solve two additional platinum derivatives [K₂PtI₄, K₂Pt(NH₃)₂(NO₃)₂] by difference Fourier, indicating three and four sites respectively at low resolution. The handedness was determined by applying the initial SIRAS phases for both enantiomers to one of the Platinum derivatives. Heavy atom sites, including symmetry copies, were examined

for the presence of non-crystallographic symmetry. This indicated the presence of three monomers in the asymmetric unit; two related by a non-crystallographic 2-fold, the third being part of a crystallographic dimer. Examination of other lanthanide derivatives (Tb and Eu) revealed the same sites but the Eu derivative gave somewhat better phasing statistics than the original SmCl_3 derivative. Final heavy atom parameters used for phasing were obtained by a Dickerson-type refinement (Dickerson *et al.*, 1968) as implemented in the CCP4 program PHASE. Isomorphous and anomalous differences of EuCl_3 (five sites, 3 days soak at 0.3 mg/ml) were used for phasing to 3.2 Å resolution, isomorphous differences of K_2PtI_4 (three sites, 2 days soak at 0.5 mg/ml) contributed to a spacing of 5.0 Å. The quality of the resulting electron density map was further improved by the application of solvent flattening techniques (Wang, 1985). Three cycles of density modification and phase combination lead to an interpretable electron density map.

Acknowledgements

We are very much indebted to Dr M. Pech for stimulating discussions and critical reading of the manuscript and thank Dr B. Wipf for large scale fermentation. The coordinates of PDGF-BB have been deposited in the Brookhaven Protein Databank.

References

- Antoniades, H.N., Scher, C.D. and Stiles, C.D. (1979) *Proc. Natl. Acad. Sci. USA*, **76**, 1809.
 Bowen-Pope, D.F. and Ross, R. (1982) *J. Biol. Chem.*, **257**, 5161–5171.
 Clements, X. *et al.* (1991) *EMBO J.*, **10**, 4113–4120.
 Deuel, T.F., Huang, J.S., Proffitt, R.T., Baenziger, J.U., Chang, D. and Kennedy, B.B. (1981) *J. Biol. Chem.*, **256**, 8896–8899.
 Deuel, T.F., Huang, J.S., Huang, S.S., Stroobant, P. and Waterfield, M.D. (1983) *Science*, **221**, 1348–1350.
 Dickerson, R.E., Weinzierl, J.E. and Palmer, R.A. (1968) *Acta crystallogr., B24*, 997–1001.
 Dolittle, R.F., Hunkapiller, M.W., Hood, L.E., Devare, S.G., Robbins, K.C., Aaronson, S.A. and Antoniades, H.N. (1983) *Science*, **221**, 275–277.
 Drozdoff, V. and Pledger, W.J. (1991) *J. Biol. Chem.*, **266**, 17165–17172.
 Garrett, J.S., Coughlin, S.R., Niman, H.L., Tremble, P.M., Giels, G.M. and Williams, L.T. (1984) *Proc. Natl. Acad. Sci. USA*, **81**, 7466–7470.
 Gelmann, E.P., Wong-Staal, F., Kramer, R.A. and Gallo, R.C. (1981) *Proc. Natl. Acad. Sci. USA*, **78**, 3373.
 Giese, N.A., Robbins, K.C. and Aaronson, S.A. (1987) *Science*, **236**, 1315–1318.
 Giese, N., LaRochelle, W.J., May-Siroff, M., Robbins, K.C. and Aaronson, S.A. (1990) *Mol. Cell. Biol.*, **10**, 5496–5501.
 Gordon, A., Ferns, A., Raines, W., Sprugel, K.H., Motani, A.S., Reidy, M. and Ross, R. (1991) *Science*, **253**, 1129–1132.
 Heideran, M.A., Pierce, J.H., Yu, J.-C., Lombardi, D., Artrip, J.E., Fleming, T.P., Thomason, A. and Aaronson, S.A. (1991) *J. Biol. Chem.*, **266**, 20232–20237.
 Heldin, C.-H. and Westmark, B. (1984) *Cell*, **37**, 9–20.
 Heldin, C.-H. and Westmark, B. (1989) *Trends Genet.*, **5**, 108–111.
 Heldin, C.-H., Westmark, B. and Wasteson, A. (1979) *Proc. Natl. Acad. Sci. USA*, **76**, 3722.
 Hendrickson, W.A. and Konnert, J.H. (1980) In Diamond, R., Ramaseshan, S. and Venkatesan, K. (eds) *Computing in Crystallography*. Indian Institute of Science, Bangalore 13.01–13.23.
 Huang, J.S., Huang, S.S., Kennedy, B. and Deuel, T.F. (1982) *J. Biol. Chem.*, **257**, 8130–8136.
 Huang, J.S., Huang, S.S. and Deuel, T.F. (1984) *Cell*, **39**, 79–97.
 Johnsson, A., Heldin, C.-H., Westmark, B. and Wasteson, A. (1982) *Biochem. Biophys. Res. Commun.*, **104**, 66–71.
 Josephs, S.F., Ratner, L., Clarke, M.F., Westin, E.H., Reitz, M.S. and Wong-Staal, F. (1984) *Science*, **225**, 636–639.
 Kabsch, W. (1988) *J. Appl. Crystallogr.*, **21**, 916–924.
 Kabsch, W. and Sander, C. (1983) *Biopolymers*, **27**, 2577–2637.
 Kanakaraj, P., Raj, S., Khan, S.A. and Bishayee, S. (1991) *Biochemistry*, **30**, 1761–1767.
 Kaplan, D.K., Chao, F.C., Stiles, C.D., Antoniades, H.N. and Scher, C.D. (1979) *Blood*, **53**, 1043.
 Kelly, J.D., Raines, E.W., Ross, R. and Murray, M.J. (1985) *EMBO J.*, **4**, 3399–3405.
 Kohler, N. and Lipton, A. (1974) *Exp. Cell. Res.*, **87**, 297–301.
 LaRochelle, W., Robbins, K.C. and Aaronson, S.A. (1989) *Mol. Cell. Biol.*, **9**, 3538–3542.
 LaRochelle, W.J., Giese, N., May-Siroff, M., Robbins, K.C. and Aaronson, S.A. (1990) *Science*, **248**, 1541–1544.
 Le Nguyen, D., Heitz, A., Chiche, L., Castro, B., Boigegrain, R.A., Favel and Coletti-Previero, M.A. (1990) *Biochimie*, **72**, 431–435.
 Matsui, T., Heidaran, M., Miki, T., Popescu, N., LaRochelle, W., Kraus, M., Pierce, J. and Aaronson, S. (1989) *Science*, **243**, 800–804.
 McDonald, N.Q., Lapatto, R., Murray-Rust, J., Gunning, J., Wlodawer, A. and Blundell, T.L. (1991) *Nature*, **354**, 422–424.
 McPherson, A. (1976) *Methods Biochem. Anal.*, **23**, 249–345.
 Nishiuchi, Y., Kumagaye, K., Noda, Y., Watanabe, T.X. and Sakakibara, S. (1986) *Biopolymers*, **25**, S61–S68.
 Owen, A.J., Pantazis, P. and Antoniades, H.N. (1984) *Science*, **225**, 54–56.
 Östman, A., Andersson, M., Hellman, U. and Hedin, C.-H. (1991) *J. Biol. Chem.*, **266**, 10073–10077.
 Priestle, J.P. (1988) *J. Appl. Crystallogr.*, **21**, 572–576.
 Rees, D.C. and Lipscomb, W.N. (1982) *J. Mol. Biol.*, **160**, 475–498.
 Robbins, K.C., Devare, S.G. and Aaronson, S.A. (1981) *Proc. Natl. Acad. Sci. USA*, **78**, 2918.
 Robbins, K.C., Hill, R.L. and Aaronson, S.A. (1982a) *Virology*, **41**, 721.
 Robbins, K.C., Devare, S.G., Reddy, E.P. and Aaronson, S.A. (1982b) *Science*, **218**, 1131.
 Ross, R., Glomset, J.A., Kariya, B. and Harker, L. (1974) *Proc. Natl. Acad. Sci. USA*, **71**, 1207–1210.
 Ross, R., Raines, R.R. and Bowen-Pope, D.F. (1986) *Cell*, **46**, 155–169.
 Sauer, M.K. and Donoghue, D.J. (1988) *Mol. Cell. Biol.*, **8**, 1011–1018.
 Seifert, R.A., Hart, C.E., Phillips, P.E., Forstrom, J.W., Ross, R., Murray, M.J. and Bowen-Pope, D.F. (1989) *J. Biol. Chem.*, **264**, 8771–8778.
 Sheriff, S. and Hendrickson, W.A. (1987) *Acta Crystallogr., A43*, 118–121.
 Theilen, G.H., Gould, D., Fowler, M. and Dungworth, D.L. (1971) *J. Natl. Cancer Inst.*, **47**, 881–889.
 Wang, B.C. (1985) *Methods Enzymol.*, **115**, 90.
 Waterfield, M.D. *et al.* (1983) *Nature*, **304**, 35–39.
 Wong-Staal, F., Favera, R.D., Gelmann, E.P., Manzari, V., Szala, S., Josephs, S.F. and Gallo, R.C. (1981) *Nature*, **294**, 273–275.
 Yarden, Y. *et al.* (1986) *Nature*, **323**, 226–232.

Received on 22 May, 1992; revised on 20 July, 1992